

# The enhancement of current and efficiency in feedback coupled Brownian ratchets

Tian-fu Gao<sup>1</sup>, Bao-quan Ai<sup>2</sup>, Zhi-gang Zheng<sup>3</sup>  
and Jin-can Chen<sup>4</sup>

<sup>1</sup> College of Physical Science and Technology, Shenyang Normal University, Shenyang 110034, People's Republic of China

<sup>2</sup> Laboratory of Quantum Engineering and Quantum Materials, School of Physics and Telecommunication Engineering, South China Normal University, Guangzhou 510006, People's Republic of China

<sup>3</sup> College of Information Science and Engineering, Huaqiao University, Xiamen 361021, People's Republic of China

<sup>4</sup> Department of Physics, Xiamen University, Xiamen 361005, People's Republic of China

E-mail: [zgzheng@hqu.edu.cn](mailto:zgzheng@hqu.edu.cn) and [jcchen@xmu.edu.cn](mailto:jcchen@xmu.edu.cn)

Received 31 May 2016, revised 5 August 2016

Accepted for publication 5 August 2016

Published 12 September 2016

Online at [stacks.iop.org/JSTAT/2016/093204](http://stacks.iop.org/JSTAT/2016/093204)  
[doi:10.1088/1742-5468/2016/09/093204](https://doi.org/10.1088/1742-5468/2016/09/093204)



CrossMark

**Abstract.** Traditionally, time delay in overdamped Brownian ratchet systems reduces the rectified transport. Strikingly, in our delayed feedback ratchets, which are alternatively switched on and off in dependence of the state of the system, time delay can have significant positive-effects that the average velocity of the coupled ratchets are improved with the presence of the delayed time. Moreover, the anomalous transport can arise and then the negative mobility phenomenon appears by changing the bias force. Meanwhile, the bias force  $F$  can facilitate Stokes efficiency of delayed feedback ratchets in the anomalous transport region. Remarkably, it is interesting to find that the coupled ratchets can acquire a series of resonant steps that are induced by frequency locking. More importantly, the optimal delay time can also facilitate Stokes efficiency. The theoretical results may provide a new operating technique in which micro- and nano-motor performance could be improved by the state or information of the delayed feedback coupled ratchets.

**Keywords:** Brownian motion, fluctuation phenomena, stochastic particle dynamics, transport properties

---

**Contents**

<b>1. Introduction</b>	<b>2</b>
<b>2. Delayed feedback ratchets for coupled inertial Brownian particles</b>	<b>3</b>
<b>3. Current and efficiency of delayed feedback ratchets</b>	<b>5</b>
<b>4. Simulations of inertial delayed-feedback Langevin equations</b>	<b>6</b>
4.1. Current and diffusion versus external force . . . . .	7
4.2. Current and diffusion versus delay time . . . . .	9
4.3. Resonant steps in delayed-feedback ratchets . . . . .	11
4.4. Current efficiency . . . . .	11
<b>5. Concluding remarks</b>	<b>14</b>
<b>Acknowledgments</b>	<b>15</b>
<b>References</b>	<b>15</b>

---

**1. Introduction**

The transport of Brownian particles under zero-average forces, i.e. ratchet transport, has been extensively investigated in the last two decades [1, 2]. Moreover, this phenomenon has also been observed in the experiments and simulations of nonlinear systems, where spatiotemporal symmetries have been properly broken. In particular, the ratchet models were used to elucidate the working principles of molecular motors, design molecular motors [3], and explain the unidirectional motion of fluxons in Josephson junctions [4], the transport of cold atoms in optical lattices [5], the vortices in superconductors [6] and the granular systems realized in experiments [7, 8].

More recently, there has been a rapid development of various artificial nanomotors with the aim of mimicking the performance of biological machines [9]. Because an external feedback of the system state is often needed to operate the system, the goal is to design autonomous machines that operate under steady-state conditions in analogy to their biological counterparts. Since motor proteins often function collectively in the cell, a detailed understanding of the molecular motor function requires considering the role of cooperative effects mediated through, excluded volume interactions or mechanical constraints imposed by motors being coupled to the same cargo [10]. Likewise, man-made molecular motors must operate in unison in order to achieve the desired efficiency and fidelity [11]. Therefore, it is necessary to consider the coupled effect for many-body motor systems.

Besides the dynamics itself, another topic of intense research is the impact of feedback control on nonequilibrium ratchet systems [12]. Although many earlier studies of

feedback-controlled systems focused on *instantaneous* feedback (i.e. no time lag between the measurement and the control action) [13], there is increasing interest in exploring systems with time delay [14–16]. The latter typically arises from a time lag between the detection of a signal and the control action, an essentially omnipresent situation in experimental setups. Exploring these ideas is fostered by recent advancements of experimental techniques for single-particle manipulation and electronic transport, which is of major relevance in various areas such as microfluidics [17], biomedical engineering [18] and quantum optics [19].

Our aim is to demonstrate that directed ratchet transport can be enhanced with the application of a time-delayed feedback control in coupled Brownian ratchets. Recently, in the context of controlling transport in the Brownian ratchet, a feedback strategy was successfully utilized for two ratchet systems interacting through a unidirectional delay coupling [20]. But, for most of them, the effects of time-delayed feedback on the rectification of thermal motion of Brownian ratchets were studied in overdamped systems [21–24]. A recent experimental implementation using such a feedback mechanism for a flashing ratchet was realized with an optical line trap and it was observed that the use of feedback increases the ratchet velocity up to an order of magnitude [25], which is in agreement with theoretical results. However, in this paper, time delay can have the significant positive effects in inertial coupled Brownian ratchets. For example, it can improve the current and corresponding performance and generate new effects, such as anomalous transport and resonant steps in our time-delayed feedback coupled ratchets.

Of particular interest for evaluating how feedback coupled ratchets work effectively, the efficiency is an important measure. In the case of Brownian ratchets, how is the efficiency to be defined? So far, the efficiency is generally defined as the ratio of the work done by the particle against the load to the input energy [26–28]. Importantly, at external force  $F = 0$  it is the addend in question that represents the only useful work produced by the motor and thus prevents the efficiency from becoming zero. Motivated by this point, Derenyi *et al* [29] proposed a new efficiency definition which does not recourse to the external load. In what follows, we call this quantity the generalized efficiency so as to emphasize its more general behavior. Thus, the generalized efficiency differs from the conventional one. That is, a task is first specified, i.e. to translocate the motor over a distance  $L$  during a given time  $t$ , and the efficiency is defined as the ratio of the minimum energy necessary for the task to the input energy.

Our investigation is based on an inertial noise-driven feedback coupled Brownian ratchet. In this work, we will concentrate on the transport properties in inertia ratchet systems via time-delayed feedback as well as the performance characteristics in flashing ratchets when the potential is alternatively switched on and off depending on the state of the system. The connection between the diffusion and the velocity fluctuations and the optimization of Stokes efficiency are also considered.

## 2. Delayed feedback ratchets for coupled inertial Brownian particles

We consider the motion of two Brownian particles at temperature  $T$  in a 1D asymmetric periodic potential  $V(x)$ , as shown in figure 1, where  $x$  is the position of the particle.

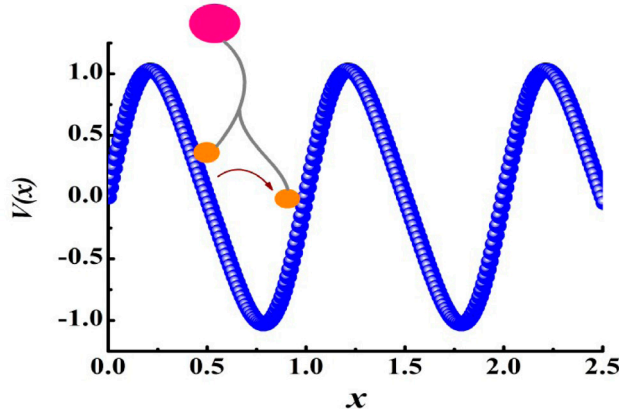


**Figure 1.** Schematic diagram of coupled Brownian particles in the ratchet potential  $V(x)$ .

The two Brownian particles interact with the underlying structure of the track (reminiscent of a microtubular trail for kinesins) via a ratchet potential  $V(x)$  [30],

$$V(x) = \sin\left(\frac{2\pi x}{L}\right) + \frac{\Delta}{4} \sin\left(\frac{4\pi x}{L}\right), \quad (1)$$

where  $\Delta$  is the asymmetry parameter of the potential. In equation (1), we set the period  $L = 1$ . It is easily seen that this potential is asymmetric. According to Curie's principle, the net directed flux in a particular direction can only occur if there is a symmetry-breaking feature in the setup. In our case, the symmetry-breaking feature is the asymmetry of the potential  $V(x)$ .

The feedback ratchets are coupled by a harmonic spring of a natural length  $l$  and an elasticity constant  $k$ . Meanwhile, the two particles are subjected to an external *unbiased* time-periodic force  $A \cos \omega t$  with angular frequency  $\omega$  and amplitude strength  $A$ . The constant bias force  $F$  acting on particles is also applied. Therefore, the stochastic dynamics of the inertial coupled ratchets with delay time is described by the following (dimensionless) Langevin equations:

$$\ddot{x}_1 + \gamma \dot{x}_1 = -\alpha(t)V'(x_1) + k(x_2 - x_1 - l) + A \cos \omega t - F + \sqrt{2\gamma D}\xi_1(t), \quad (2)$$

and

$$\ddot{x}_2 + \gamma \dot{x}_2 = -\alpha(t)V'(x_2) - k(x_2 - x_1 - l) + A \cos \omega t - F + \sqrt{2\gamma D}\xi_2(t), \quad (3)$$

where the dot and the prime denote a differential with respect to the time  $t$  and the space coordinate  $x$  of the Brownian particles, respectively, and the parameter  $\gamma$  characterizes the friction coefficient.  $\xi_i(t)$  ( $i = 1, 2$ ) are the Gaussian white noise with  $\langle \xi_i(t) \rangle = 0$  and  $\langle \xi_i(t)\xi_j(s) \rangle = \delta_{ij}\delta(t-s)$ . The symbol  $\langle \dots \rangle$  denotes an ensemble average over the distribution of the independent random forces.  $D$  is the noise intensity. The switch of ratchet potential  $V(x)$  is determined by the controller  $\alpha(t)$ .

The main feature of our driving mechanism, which was not considered in [31], is the presence of a time delay,  $\tau$ . As discussed in several studies (e.g. [21–24, 32]), time delay is a rather natural phenomenon which may arise, e.g. through the finite time required for measuring or processing information from a measurement. The controller  $\alpha(t)$  is

determined by the sign of the *average force*  $f(t)$  [21–24], and after a time  $\tau$ , switches the potential on ( $\alpha = 1$ ) if the ensemble average of the force is positive or switches the potential off ( $\alpha = 0$ ) if it is negative. This delayed feedback control protocol can be expressed as

$$\alpha(t) = \begin{cases} \Theta(f(t - \tau)), & t \geq \tau \\ 0, & \text{otherwise} \end{cases}, \quad (4)$$

where  $\Theta$  is the Heaviside function. Therefore, the alternative controller  $\alpha(t)$  in equation (4) is only dependent on the internal state of the coupled Brownian ratchets. As ‘control target’ we consider the average force  $f(t)$  due to the potential switch on,

$$f(t) = \frac{1}{2} \sum_{i=1}^2 F_{\text{pot}}(x_i(t)) = -\frac{1}{2} [V'(x_1(t)) + V'(x_2(t))]. \quad (5)$$

Thus, the average force applies the delayed feedback control onto the coupled ratchets.

### 3. Current and efficiency of delayed feedback ratchets

The most important quantity characterizing coupled Brownian ratchets is its directed center-of-mass mean velocity [31]

$$\langle V_{\text{cm}} \rangle = \lim_{t \rightarrow \infty} \frac{1}{2} \frac{\omega}{2\pi} \sum_{i=1}^2 \int_t^{t+2\pi/\omega} \langle \dot{x}_i(s) \rangle ds, \quad (6)$$

where  $\langle \dots \rangle$  indicates the average over initial conditions and thermal noise realizations (ensemble average).

Although particles may be diffusive at all times, a time-dependent average effective diffusion coefficient  $D_{\text{eff}}$  can be defined as [33]

$$D_{\text{eff}} = \lim_{t \rightarrow \infty} \frac{1}{2} \sum_{i=1}^2 \frac{\langle x_i(s)^2 \rangle - \langle x_i(s) \rangle^2}{2t}. \quad (7)$$

The average effective diffusion coefficient describes the fluctuations around the average position of the coupled Brownian particles. Intuitively, if the stationary velocity is large and the spread of trajectories is small, the diffusion coefficient is small and the directed transport is more effective.

Of equal importance are, however, the fluctuations of center-of-mass velocity  $V_{\text{cm}}(t)$  around its mean  $\langle V_{\text{cm}} \rangle$  in the long-time regime, i.e. the variance [31, 34]

$$\sigma_v^2 = \langle V_{\text{cm}}^2 \rangle - \langle V_{\text{cm}} \rangle^2. \quad (8)$$

The coupled Brownian ratchets move with the center-of-mass velocity  $V_{\text{cm}}(t)$  that ranges typically within

$$V_{\text{cm}}(t) \in (\langle V_{\text{cm}} \rangle - \sigma_v, \langle V_{\text{cm}} \rangle + \sigma_v). \quad (9)$$

If  $\sigma_v > \langle V_{\text{cm}} \rangle$ , the coupled particles can possibly move for some time in the opposite direction of its average value  $\langle V_{\text{cm}} \rangle$ .

We have also examined the efficiency of the energy transformation following the method in [34], which also yields a non-vanishing rectification efficiency in the absence of an external bias. This efficiency of rectification follows from an energy balance of the underlying inertial Langevin dynamics. When specialized to Brownian ratchets, the efficiency, namely its *Stokes efficiency*  $\eta_s$ , is given by the ratio of the dissipated power  $\gamma \langle V \rangle^2$  associated with the directed motion against friction to the input power  $P_{\text{in}}$  from the time-periodic forcing [31, 35]. As coupled Brownian ratchets, we replace the average velocity  $\langle V \rangle$  in [31, 35] by the center-of-mass mean velocity  $\langle V_{\text{cm}} \rangle$  to obtain the *Stokes efficiency*,

$$\eta_s = \frac{\gamma \langle V_{\text{cm}} \rangle^2}{P_{\text{in}}} = \frac{\langle V_{\text{cm}} \rangle^2}{\langle V_{\text{cm}}^2 \rangle - D} = \frac{\langle V_{\text{cm}} \rangle^2}{\langle V_{\text{cm}} \rangle^2 + \sigma_v^2 - D}. \quad (10)$$

It thus follows that for a decreasing variance of the center-of-mass velocity fluctuations,  $\sigma_v^2$ , the Stokes efficiency of the coupled ratchets increases. This is just what one would expect on naive grounds. The transport of delayed feedback ratchets can be optimized in the regime of a large directed average current which intrinsically exhibits only small fluctuations. Moreover, in coupled Brownian ratchets, it is also found numerically that  $\langle V_{\text{cm}}^2 \rangle > D$  holds true for any chosen set of the simulation parameters. In the next section, we will demonstrate that the time delay is indeed *crucial* for the enhancement of the coupled ratchets transport.

#### 4. Simulations of inertial delayed-feedback Langevin equations

Focusing on the mean velocity, we investigate the asymptotic time-periodic regime after the effects of the initial conditions and transient processes have died out. Then, the statistical quantifiers of interest can be determined in terms of the statistical average over the different realizations of the processes in equations (2) and (3) and over the driving period  $T_\omega$ .

The feedback properties of coupled Brownian ratchets in typical molecular motors, like kinesins, have been formerly addressed in experimental studies and inertial Langevin dynamics simulations. Clearly, there exist no analytical methods of analyzing equations (2) and (3) in the presence of inertia. Therefore, we performed extensive numerical studies by employing the second order Stochastic Runge–Kutta (SRK) algorithm with a time step  $h = 10^{-3}$ . The initial conditions for the position  $x(t_0)$  were chosen according to a random distribution over the periodic  $L$  of the ratchet potential given in equation (1). The initial velocities  $v(t_0)$  were randomly chosen from a uniform distribution over the interval  $[-0.2, 0.2]$ . All quantities were averaged over 500 different trajectories, each of which evolved over  $5 \times 10^4$  driving-periods  $T_\omega$ . For the investigation of the current efficiency defined above, we restrict the discussion here to a set of driving parameters, reading,  $L = 1$ ,  $\gamma = 1.546$ ,  $\Delta = 0.05$ ,  $k = 0.01$ ,  $l = 0.1$ .

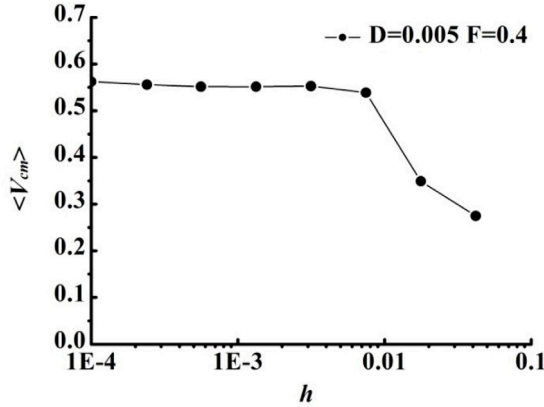


**Figure 2.** The curve of the center-of-mass average velocity  $\langle V_{\text{cm}} \rangle$  varying with the time step  $h$  for noise intensity  $D = 0.005$  and the bias force  $F = 0.4$ , where  $\tau = 0.12$ ,  $A = 8.95$  and  $\omega = 3.77$ .

In this work we have considered the SRK algorithm for solving the stochastic differential equations of the delayed-feedback ratchets. To further illustrate the algorithmic efficiency at different time steps, we depict the asymptotic center-of-mass average velocity  $\langle V_{\text{cm}} \rangle$  as a function of time step  $h$ , as shown in figure 2. It is found that the curve of the center-of-mass average velocity varying with the time step is nearly flat for the time step  $h < 10^{-2}$ , and then the curve is convergent until the time step  $h \rightarrow 0.1$ . It is apparent that the second order Runge–Kutta algorithm provides useful information on the maximum value of time step and  $h$  of our SRK algorithm can be properly used, enabling us to choose a suitable time step  $h = 10^{-3}$  for numerical simulations.

#### 4.1. Current and diffusion versus external force

In figure 3(a) we depict the force–velocity characteristics of the feedback coupled Brownian ratchets, for different values of the delay time  $\tau$ . Contrary to the familiar, usually monotonic dependence found for our overdamped ratchets dynamics [36], now the velocity–force behavior becomes more complex, exhibiting distinct non-monotonic characteristics in the present of delay time. This figure clearly shows that the delayed feedback ratchets exhibit the behaviors of *anomalous transport* that a very weak negative driving (negative bias forces in equations (2) and (3)) yields a positive center-of-mass average velocity ( $\langle V_{\text{cm}} \rangle > 0$ ) in the case of feedback control  $\tau \neq 0$ . It can be seen that the feedback ratchets can proceed with a large positive velocity for  $\tau = 0.03$  within a large interval of the bias  $F$ . Even when the delay time increases to 0.1, the *anomalous transport* still exists. However, the feedback ratchets display normal transport ( $\langle V_{\text{cm}} \rangle < 0$ ) by further increasing bias force  $F$ . Therefore, the *anomalous transport* is also obtained from inertial feedback coupled ratchets which are different from the previous conclusion [36]. More importantly, the value of  $\langle V_{\text{cm}} \rangle$  for  $\tau \neq 0$  is larger than that for  $\tau = 0$ , which means that the delay time can enhance the transport of inertial feedback ratchets. It can be clearly obtained that the center-of-mass average velocity also depends on delay time  $\tau$ . This phenomenon will be discussed in the next section.

Specially, if there is no delayed feedback control, i.e.  $\tau = 0$ , a typical *anomalous transport* phenomenon is also presented in figure 3(a) (see the inset). The average

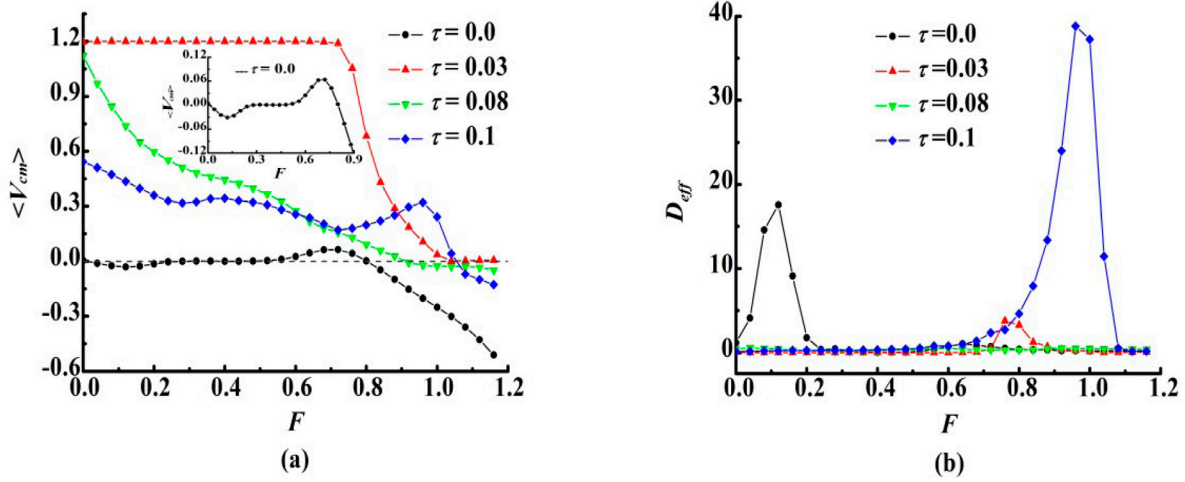


**Figure 3.** The curves of (a) the center-of-mass average velocity  $\langle V_{cm} \rangle$  and (b) the average effective diffusion coefficient  $D_{eff}$  varying with the bias force  $F$  for different values of the time delay  $\tau$ , where  $D = 0.001$ ,  $A = 8.95$  and  $\omega = 3.77$ .

velocity  $\langle V_{cm} \rangle \rightarrow 0$  for small bias force  $F$ , which means that the system is at a locked state that does not contribute to the directed transport [37]. For  $\tau = 0$ , the velocity  $\langle V_{cm} \rangle$  is negative versus small negative  $F$ . Upon further increasing the bias, the velocity  $\langle V_{cm} \rangle$  changes sign, takes a positive maximum value, and then reverses direction again, which means the emergence of the negative nonlinear mobility (NNM) phenomenon [38] (the transport direction follows the small bias force, but changes sign and switches to the opposite direction upon further increasing the bias). However, the NNM disappears, after that the velocity against the bias shows the character of normal transport with  $F > 0.8$ . In this progress, the particles display abnormal motion firstly and then normal motion, which means that the current of coupled Brownian ratchets reversals for two times.

The average effective diffusion coefficient  $D_{eff}$  against the external bias  $F$  is plotted in figure 3(b) within a particular parameter space. It is found that the  $D_{eff}-F$  behavior becomes more complex. For different values of the delay time  $\tau$ ,  $D_{eff}$  exhibits one or multi-maximum values, which means that one or multi-optimal bias forces  $F^{opt}$  can facilitate the diffusion of coupled Brownian ratchets in the case of anomalous transport region.

In figure 4(a), we depict the asymptotic center-of-mass average velocity  $\langle V_{cm} \rangle$  as a function of the bias force  $F$  for different values of the noise intensity  $D$  at delay time  $\tau = 0.12$ . A typical example for the *anomalous transport* phenomenon where particles always move in a direction opposite to the net acting force is displayed. It is interesting to find that the velocity  $\langle V_{cm} \rangle$  has positive-valued maxima at different optimal values  $F^{opt}$  of the bias force for noise intensity  $D < 0.1$ , which means that the positive velocity can be maximized by choosing the proper noise intensity and external bias force for our delayed feedback ratchets. However, the peak can be explained by the negative mobility (NM) effect [39–41]. The result is similar to that obtained for non-feedback Brownian ratchet in figure 1 of [30]. However, as the noise intensity is increased, e.g.  $D = 0.1$ , the peaks disappear and  $\langle V_{cm} \rangle$  decreases monotonically with the increase of the

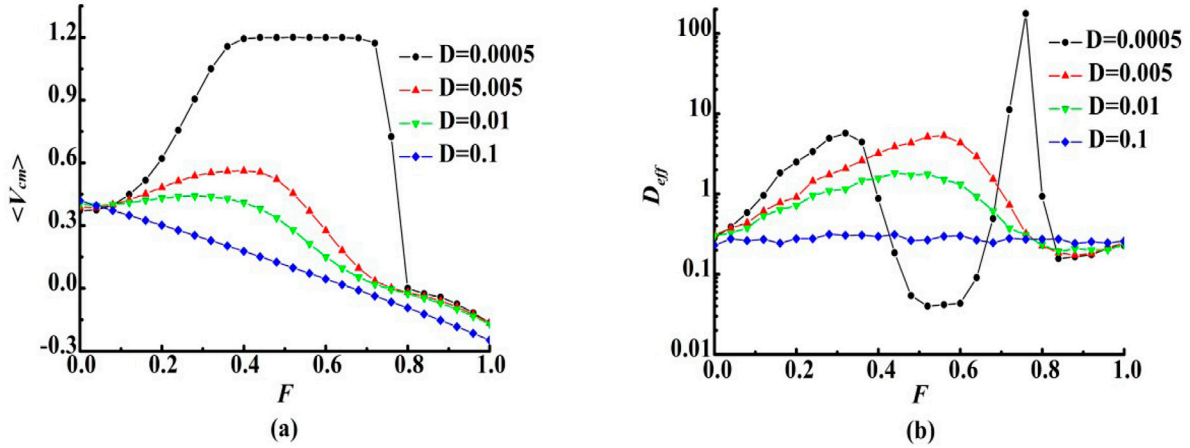


**Figure 4.** The curves of (a) the center-of-mass average velocity  $\langle V_{cm} \rangle$  and (b) the average effective diffusion coefficient  $D_{eff}$  varying with the bias force  $F$  for different values of the noise intensity  $D$ , where  $\tau = 0.12$ ,  $A = 8.95$  and  $\omega = 3.77$ .

bias force. It can be understood that in this case, the negative mobility effect disappears, the noise driving ratchet effect increases, and consequently, the transport is dominated by the noise effect.

In order to understand the phenomenon deeply, we calculate the average effective diffusion coefficient  $D_{eff}$  as a function of the bias force  $F$  for different values of the noise intensity  $D$ , as shown in figure 4(b). It can be easily seen that there are two peaks for small noise intensity  $D = 0.0005$ , which means that in the case of low temperature (small noise intensity), the coupled Brownian ratchets are more easy to diffuse at the respective optima bias  $F^{opt}$ . However, the peak decreases to one and its height also decreases when the temperature of the feedback ratchets is increased and  $D$  ranges from 0.005 to 0.01. In the anomalous transport region of  $D < 0.1$ , no matter what the noise intensity  $D$  is, the optimal bias forces  $F^{opt}$  can facilitate the diffusion of coupled Brownian ratchets. But for the high temperature case of  $D = 0.1$ , the diffusion coefficient  $D_{eff}$  does not vary obviously with the increase of the bias force, and consequently, it is difficult for the diffusion of coupled ratchets in the case of high temperature. It can be understood that with the increase of the noise intensity (temperature), the fluctuation of displacement of coupled particles decreases, and therefore  $D_{eff}$  decreases drastically.

#### 4.2. Current and diffusion versus delay time

In figure 5(a), we display the influence of the delay time  $\tau$  of the feedback ratchets on the center-of-mass average velocity  $\langle V_{cm} \rangle$  for different values of the amplitude  $A$ . Moreover, the simulations are done at fixed force  $F = 0.3$ . In the case of  $A = 0$ , only the external force  $F$  can help the particle to cross the ratchet potential  $V(x)$ . When the bias  $F = 0.3$ , the particles cannot overcome the potential well, and therefore the effect of the delay time  $\tau$  on the mean velocity  $\langle V_{cm} \rangle$  disappears for amplitude  $A = 0$ . Nevertheless, it is demonstrated in figure 5(a) that  $\langle V_{cm} \rangle$  as a function of delay time  $\tau$  becomes more complex for driving amplitude  $A \neq 0$ . It is clearly seen that the velocity  $\langle V_{cm} \rangle$  has the maxima value at an optimal value  $\tau^{opt}$  of the delay time for amplitude  $A = 2.5$ . This

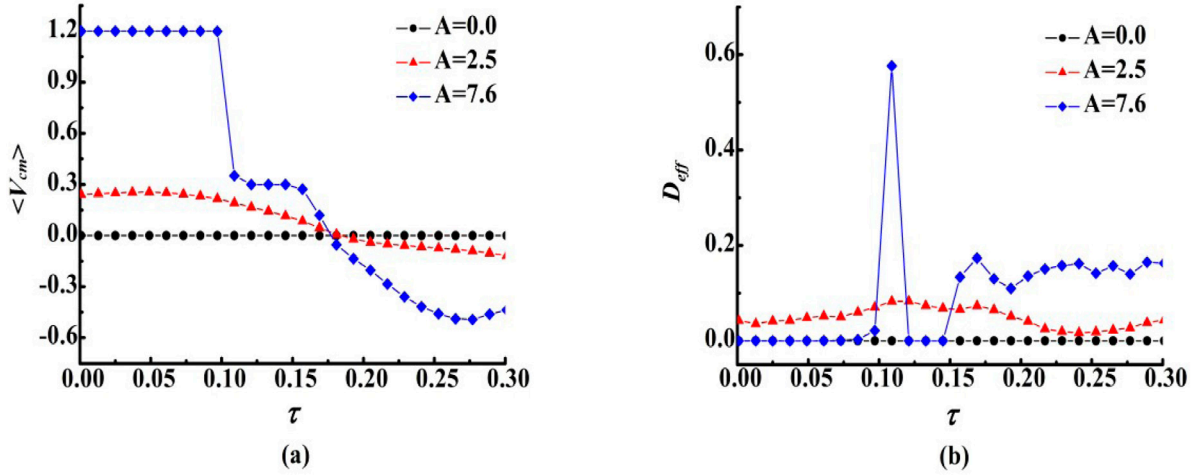


**Figure 5.** The curves of (a) the center-of-mass average velocity  $\langle V_{cm} \rangle$  and (b) the average effective diffusion coefficient  $D_{eff}$  varying with the time delay  $\tau$  for different values of the amplitude  $A$ , where  $D = 0.001$ ,  $F = 0.3$  and  $\omega = 3.77$ .

means that the transport can be maximized by choosing the proper delay time and amplitude of the periodic driving for our delayed feedback ratchets. However, when the driving amplitude is increased, e.g.  $A = 7.6$ , it is interesting to find that this current acquires a series steps for values of the current and the value of steps are rational values. These resonant steps are due to the frequency locking in the case of external periodic driving [42], and we will discuss this resonant steps below. However, the effect of the time delay is different from the previous work in which the average velocity is a monotonically decreasing function of  $\tau$  in the case of overdamped feedback ratchets [24, 36]. It is noted that the transport can be reversed by further increasing the delay time for driving amplitude  $A \neq 0$ . In the case of large delay time, the action of the controller begins to be uncorrelated to the present state of the feedback ratchets and it effectively begins to act as an open-loop ratchet.

The effect of the delay time  $\tau$  on the average effective diffusion coefficient  $D_{eff}$  for different values of the amplitude  $A$  is shown in figure 5(b). It can be seen that the coupled particles are not easy to diffuse in the case of non-feedback ( $\tau \rightarrow 0$ ). Especially, the coupled particles are in the potential well when the driving amplitude  $A = 0$ , therefore the particles cannot diffuse freely. However, the feedback ratchets diffuse more easily at an optimal delay time  $\tau^{opt}$  for amplitude  $A = 2.5$ . If we increase the driving amplitude further, it can be seen that the average effective diffusion coefficient  $D_{eff}$  changes drastically between the different resonant steps for amplitude  $A = 7.6$ . It can be understood that the center-of-mass average velocity  $\langle V_{cm} \rangle$  of figure 5(a) for amplitude  $A = 7.6$  is nearly unchangeable at the respective region of resonant steps, implying that there is no fluctuation of displacement of coupled particles. Consequently, the coupled ratchets cannot easily diffuse and the diffusion coefficient  $D_{eff} \rightarrow 0$  at the different resonant regions, and then, there is a peak of diffusion coefficient between the different resonant regions mathematically. Nevertheless, it is easy to diffuse at the non-resonant regions for our delayed feedback ratchets, e.g. for a large delay time of  $\tau > 0.15$ .

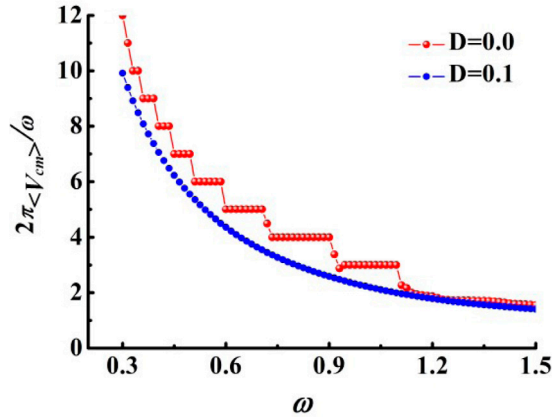


**Figure 6.** The scaled average velocity  $2\pi\langle V_{\text{cm}}\rangle/\omega$  of the delayed-feedback ratchets as a function of frequency  $\omega$  for different values of the noise intensity  $D$ . The rest of the parameters are  $A = 2.1$ ,  $F = 0.3$  and  $\tau = 0.12$ .

### 4.3. Resonant steps in delayed-feedback ratchets

Besides the driving amplitude  $A$ , the frequency of the rocking force constitutes another important source intended to influence the resonant steps. The scaled average velocity  $2\pi\langle V_{\text{cm}}\rangle/\omega$  as a function of the frequency  $\omega$  is shown in figure 6. The red line shows the deterministic case without noise and the blue line shows the stochastic case with a noise intensity of  $D = 0.1$ . For the deterministic case, we can see the successive magnifications of the resonant steps at the rational values of the flux. The scaled current can acquire a series of defined resonant steps for values of the current given by the ratio  $n/m$ , where  $n$  and  $m$  are integer numbers. In fact, the resonant steps in figure 6 can be seen as the synchronization regions under the affect of periodic driving. The detailed structure has been reported for overdamped *open-loop* ratchets in [43, 44], and for underdamped deterministic feedback ratchets [45]. Notice that the analytical prediction of resonant steps given by [45] are a series of defined steps theoretically. However, it can be observed only for a part due to the dynamics of the coupled systems in our delayed-feedback control. Furthermore, it indicates that the smaller the noise intensity is (for the deterministic case of  $D = 0.0$ ), the more the resonance step appears. As expected, in the case of  $D = 0.1$ , the scaled average velocity is a smooth curve where the structure of steps of the deterministic case disappears. Therefore the resonant steps are induced by the deterministic dynamics of coupled ratchets. However, the scaled current in this way is very large for small values of driving frequency. Mathematically, it is clear that when this driving frequency is decreased, the scaled current  $2\pi\langle V_{\text{cm}}\rangle/\omega$  increases because the center-of-mass average velocity is a finite value. Furthermore, when the external driving frequency increases, e.g.  $\omega \rightarrow \infty$ , the coupled ratchets may transport under the effect of external bias force  $-F$ , and the corresponding center-of-mass velocity decreases with the increase of frequency  $\omega$ .

### 4.4. Current efficiency

The occurrence of multiple anomalous transport of the directed current, as it occurs in figures 3(a) and 4(a), is known as the interesting feature of inertial ratchets. Several

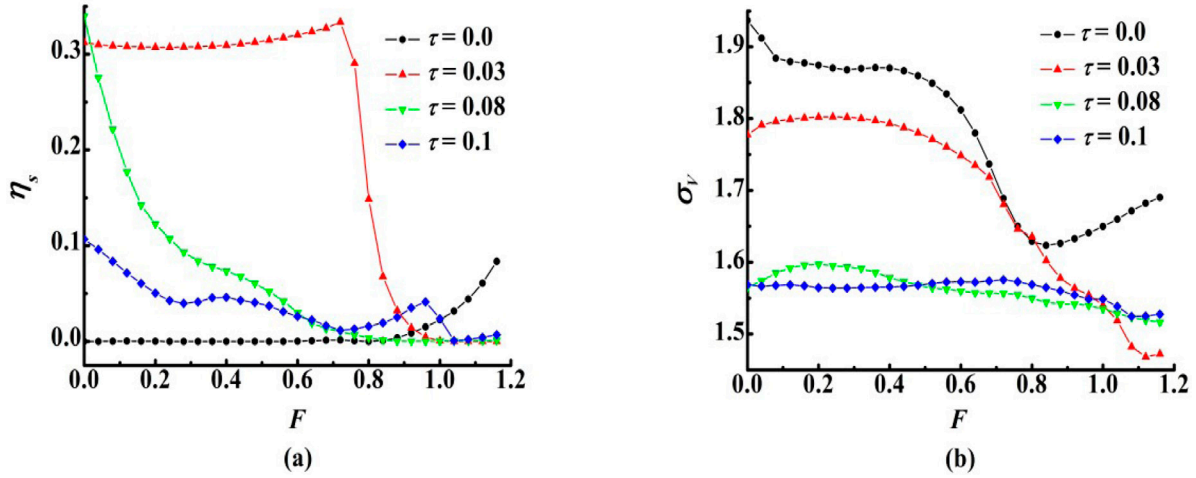


**Figure 7.** The curves of (a) the Stokes efficiency  $\eta_s$  and (b) the velocity fluctuation  $\sigma_v$  varying with the bias force  $F$  for different values of the time delay  $\tau$ , where  $D = 0.001$ ,  $A = 8.95$  and  $\omega = 3.77$ .

prior studies did elucidate in detail the corresponding mechanism about non-feedback anomalous transport [37, 38]. Here, in order to know the performance of directed transport, we take instead a closer look at the current fluctuations and efficiencies in our feedback coupled Brownian ratchets.

Figure 7 shows the curves of the Stokes efficiency  $\eta_s$  and velocity fluctuation  $\sigma_v$  varying with the bias force  $F$  for different values of time delay  $\tau$ . For the uncontrolled case of  $\tau = 0$ , the coupled ratchets cannot convert the energy efficiently and the Stokes efficiency is low, as shown in figure 7(a). It can be seen from figure 7(b) that the fluctuation of the center-of-mass average velocity  $\langle V_{cm} \rangle$  for coupled Brownian ratchets changes drastically with the increase of the bias force, and the corresponding  $\langle V_{cm} \rangle$  is small for a large interval of the bias in this case (see figure 3(a)). Therefore, the Stokes efficiency is low in the case of non-feedback.

What is needed in achieving a large rectification efficiency is a sizable coupled ratchet current or a high transport which is accompanied by small velocity fluctuations, see equation (10). When we consider the effect of the feedback, e.g. for small time delay  $\tau = 0.03$ , it can be obviously seen that the center-of-mass average velocity  $\langle V_{cm} \rangle$  is maximal for  $F < 0.9$  from figure 3(a) and we indeed find the desired enhancement of the Stokes efficiency  $\eta_s$  from figure 7(a). However, when the time delay is larger, e.g.  $\tau > 0.03$ , the velocity fluctuation  $\sigma_v$  does not vary obviously with the bias force  $F$  from figure 7(b), and  $\langle V_{cm} \rangle$  for  $\tau > 0.03$  is smaller than that  $\tau = 0.03$ , so the Stokes efficiencies decrease. Nevertheless, it is interesting to note the similar result that the Stokes efficiency  $\eta_s$  for  $\tau \neq 0$  is larger than that for  $\tau = 0$ , which also means that if we want the coupled particles to utilize the input energy more efficiently for the directional transport, the small delay time should be considered in the feedback ratchets.

Figure 8 shows the Stokes efficiency  $\eta_s$  and velocity fluctuation  $\sigma_v$  as a function of bias force  $F$  for different values of the noise intensity  $D$ . For the low temperature case of  $D = 0.0005$  in figure 8(a), it can be seen that the Stokes efficiency  $\eta_s$  can obtain a maximum value. The coupled ratchets have the high directed transport shown in figure 4(a)

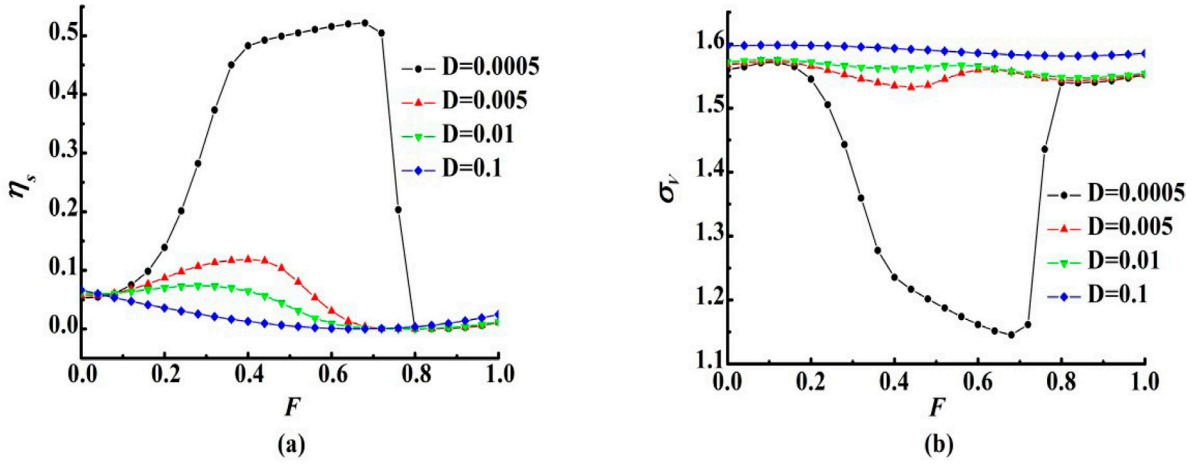


**Figure 8.** The curves of (a) the Stokes efficiency  $\eta_s$  and (b) the velocity fluctuation  $\sigma_v$  varying with the bias force  $F$  for different values of the noise intensity  $D$ , where  $\tau = 0.12$ ,  $A = 8.95$  and  $\omega = 3.77$ .

and the corresponding velocity fluctuation  $\sigma_v$  has a minimum value for bias forces, as shown in figure 8(b). However, with the increase of the noise intensity, e.g.  $D > 0.0005$ , the dissipation due to corresponding velocity fluctuation  $\sigma_v$  increases but the height of the peaks decreases for  $\langle V_{cm} \rangle$  in figure 4(a), so the Stokes efficiency  $\eta_s$  decreases and the maximum efficiency of coupled Brownian ratchets is smaller than that of coupled Brownian ratchets at low temperature cases.

In figure 8(a), it is interesting to note that  $\eta_s$  is not a monotonic function of the bias force  $F$ . For small noise intensity of  $D < 0.1$ , the Stokes efficiency  $\eta_s$  exhibits a pronounced peak, so that there is an optimal bias force  $F^{opt}$  at which  $\eta_s$  attains its maximum value  $\eta_s^{opt}$ . The stall force is around  $F_{sta} = 0.8$ . Meanwhile  $\eta_s^{opt}$  and  $F^{opt}$  decrease with the decrease of the bias force. Under the steady state case, near the stall force,  $\eta_s \rightarrow 0$ . However, the Stokes efficiencies of feedback ratchets have similar characteristic behaviors for different force–velocity relations in figure 4(a). It indicates once again that there is an optimal bias force  $F^{opt}$  to obtain more efficient transportation of the inertial feedback ratchets in the case of anomalous transport.

Figure 9 shows the Stokes efficiency  $\eta_s$  and velocity fluctuation  $\sigma_v$  as a function of time delay  $\tau$  for different values of amplitude  $A$ . It can be seen that the Stokes efficiency  $\eta_s$  has a similar complex behavior between figures 9(a) and 5(a). For the case of driving amplitude  $A = 0$ , the efficiency  $\eta_s$  tends to zero. It can be understood that there is no directed transport for this case in figure 5(a) but the velocity fluctuation  $\sigma_v$  is a non-zero finite value in figure 9(b), so that  $\eta_s \rightarrow 0$ . It can be seen from figure 5(a) that  $\langle V_{cm} \rangle$  has a maximum value at the optimal delay time  $\tau^{opt}$  for amplitude  $A = 2.5$ , but  $\sigma_v$  is nearly unchangeable in this case, seen from figure 9(b), so the Stokes efficiency  $\eta_s$  can also reach the maximum value at the optimal delay time  $\tau^{opt} = 0.05$ . However, with the increase of driving amplitude, e.g.  $A = 7.6$ , the Stokes efficiency  $\eta_s$  can obtain a maximum value and then drops drastically. The value of  $\langle V_{cm} \rangle$  is large in the first resonant step and the velocity fluctuation is decreasing during this resonant step, so the Stokes efficiency can achieve a maximum value between the two different resonant regions. However, the Stokes efficiency is small during the second resonant step and it may be

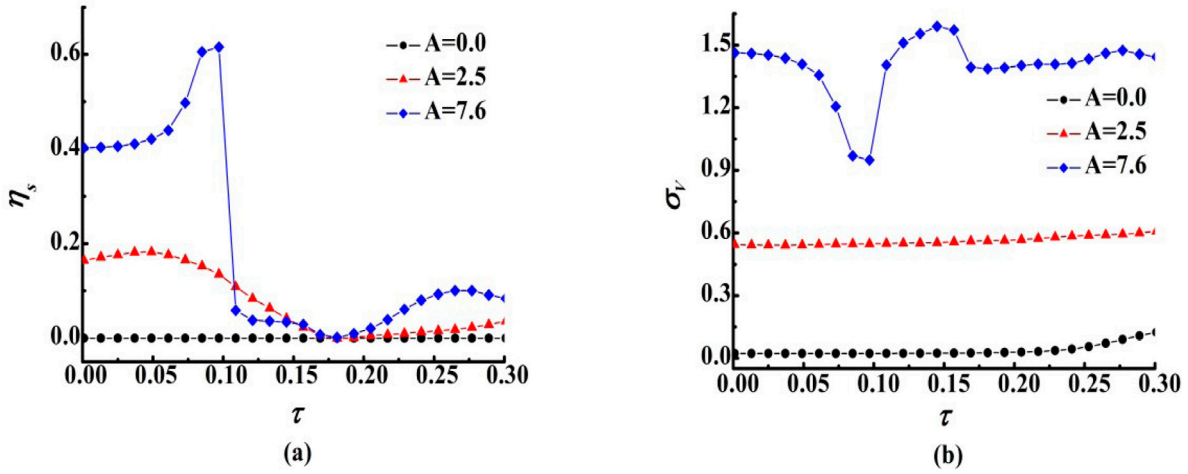


**Figure 9.** The curves of (a) the Stokes efficiency  $\eta_s$  and (b) the velocity fluctuation  $\sigma_v$  varying with the time delay  $\tau$  for different values of the amplitude  $A$ , where  $D = 0.001$ ,  $F = 0.3$  and  $\omega = 3.77$ .

deduced by analogy. Therefore, it can be understood that the efficiency enhancement may also be obtained by changing the suitable delay time and the driving amplitude.

## 5. Concluding remarks

In this work, we have studied the dynamics of coupled Brownian ratchets driven by time-periodic force and bias force and exposed to Gaussian white noise. However, the coupled Brownian ratchets are subjected to a space-dependent asymmetric potential and a time-dependent feedback control force. The control target is the time-delayed average force relative to a switching ratchet potential. To explore the transport properties of inertial feedback ratchets we have investigated the center-of-mass average velocity  $\langle V_{cm} \rangle$  and Stokes efficiency  $\eta_s$ , in dependence of several parameters such as the bias force, delayed time, noise intensity, amplitude and frequency of the driving force and so on.

It is interesting to find that for our present feedback control strategy where the potential itself is switched on and off appropriately depending on the state of the system, the time delay is *essential* for the inertial coupled Brownian ratchets and the current enhancement. A further important result is the dependence of the bias force on the center-of-mass average velocity. It is shown that the *anomalous transport* can also arise in our delayed feedback ratchets. Meanwhile, diffusion is considered in the feedback coupled system, and the bias force  $F$  can also facilitate the diffusion in *anomalous transport* region. However, the delayed feedback ratchets can acquire a series of resonant steps for different values of the current. These resonant steps are owing to the phenomenon of synchronization under the affect of periodic driving, and the steps correspond to the frequency locking. More importantly, with the increase of the delayed time, the particle current can be reversed for different driving amplitude.

However, an important question for every feedback-controlled system is its efficiency under closed-loop control. It is found that for a certain range of the bias force  $F$  and not too large delay time, the Stokes efficiency  $\eta_s$  is enhanced relative to the non-feedback control. For small noise intensity case, e.g.  $D = 0.0005$ , the Stokes efficiency is larger than that for high noise intensity cases in our feedback-controlled ratchets. Furthermore, there is an optimal bias force to obtain more efficient transportation in the anomalous transport region. However, the optimal delay time can also facilitate the Stokes efficiency. The results obtained here may inspire that the transport performance and efficiency can be controlled dynamically by the use of state or information of the feedback coupled ratchets.

## Acknowledgments

This work is supported by the National Natural Science Foundation of China (Grant No. 11475022, Grant No. 11575064, and Grant No. 11347003) and the Scientific Research Funds of Huaqiao University and the GDHVPS (2016) and the Excellent Talents Program of Shenyang Normal University (Grant No. 91400114005).

## References

- [1] Astumian R D 1997 *Science* **276** 917
- [2] Hänggi P and Marchesoni F 2009 *Rev. Mod. Phys.* **81** 387
- [3] Kay E R, Leigh D A and Zerbetto F 2007 *Angew. Chem. Int.* **46** 72
- [4] Ooi S, Savel'ev S, Gaifullin M B, Mochiku T, Hirata K and Nori F 2007 *Phys. Rev. Lett.* **99** 207003
- [5] Schiavoni M, Sanchez-Palencia L, Renzoni F and Grynberg G 2003 *Phys. Rev. Lett.* **90** 094101
- [6] Dinis L, González E M, Anguita J V, Parrondo J M R and Vicent J L 2007 *New J. Phys.* **9** 366
- [7] Gnoli A, Petri A, Dalton F, Pontuale G, Gradenigo G, Sarracino A and Puglisi A 2013 *Phys. Rev. Lett.* **110** 120601
- [8] Gnoli A, Sarracino A, Puglisi A and Petri A 2013 *Phys. Rev. E* **87** 052209
- [9] Lund K *et al* 2010 *Nature* **465** 206
- [10] Holzbaur E L F and Goldman Y E 2010 *Curr. Opin. Cell Biol.* **22** 4
- [11] Rank M, Reese L and Frey E 2013 *Phys. Rev. E* **87** 032706
- [12] Abreu D and Seifert U 2012 *Phys. Rev. Lett.* **108** 030601
- [13] Brandes T 2010 *Phys. Rev. Lett.* **105** 060602
- [14] Cao F J and Feito M 2012 *Entropy* **14** 834
- [15] Emary C 2013 *Phil. Trans. R. Soc. A* **371** 20120468
- [16] Munakata T and Rosinberg M L 2014 *Phys. Rev. Lett.* **112** 180601
- [17] Qian B, Montiel D, Bregulla A, Cichos F and Yang H 2013 *Chem. Sci.* **4** 1420
- [18] Fisher J K *et al* 2005 *Rev. Sci. Instrum.* **76** 053711
- [19] Sayrin C *et al* 2011 *Nature* **477** 73
- [20] Kostur M, Hänggi P, Talkner P and Mateos J L 2005 *Phys. Rev. E* **72** 036210
- [21] Cao F J, Dinis L and Parrondo J M R 2004 *Phys. Rev. Lett.* **93** 040603
- [22] Feito M and Cao F J 2007 *Phys. Rev. E* **76** 061113
- [23] Craig E M, Kuwada N J, Lopez B J and Linke H 2008 *Ann. Phys.* **17** 115
- [24] Feito M and Cao F J 2008 *Physica A* **387** 4553
- [25] Lopez B J, Kuwada N J, Craig E M, Long B R and Linke H 2008 *Phys. Rev. Lett.* **101** 220601
- [26] Kamegawa H, Hondou T and Takagi F 1998 *Phys. Rev. Lett.* **80** 5251
- [27] Parrondo J M R, Blanco J M, Cao F J and Brito R 1998 *Europhys. Lett.* **43** 248
- [28] Parmeggiani A, Julicher F, Ajdari A and Prost J 1999 *Phys. Rev. E* **60** 2127
- [29] Derenyi I, Bier M and Astumian R D 1999 *Phys. Rev. Lett.* **83** 903
- [30] Ai B Q and Liu L G 2007 *Phys. Rev. E* **76** 042103
- [31] Spiechowicz J, Hänggi P and Łuczka J 2014 *Phys. Rev. E* **90** 032104
- [32] Loos S A M, Gernert R and Klapp S H L 2014 *Phys. Rev. E* **89** 052136

- [33] Reimann P, Van den Broeck C, Linke H, Hänggi P, Rubi J M and Perez-Madrid A 2001 *Phys. Rev. Lett.* **87** 010602
- [34] Kostur M, Machura L, Hänggi P, Łuczka J and Talkner P 2006 *Physica A* **371** 20
- [35] Spiechowicz J, Łuczka J and Machura L 2016 *J. Stat. Mech.* **054038**
- [36] Gao T F, Zheng Z G and Chen J C 2013 *Chin. Phys. B* **22** 080502
- [37] Speer D, Eichhorn R and Reimann P 2007 *Phys. Rev. E* **76** 051110
- [38] Du L C and Mei D C 2014 *Eur. Phys. J. B* **87** 33
- [39] Eichhorn R, Reimann P and Hanggi P 2002 *Phys. Rev. Lett.* **88** 190601
- [40] Bénichou O, Illien P, Oshanin G, Sarracino A and Voituriez R 2014 *Phys. Rev. Lett.* **113** 268002
- [41] Machura L, Kostur M, Talkner P, Luczka J and Hanggi P 2007 *Phys. Rev. Lett.* **98** 040601
- [42] Alatryste F R and Mateos J L 2006 *Physica A* **372** 263
- [43] Mateos J L and Alatryste F R 2008 *Chaos* **18** 043125
- [44] Mateos J L and Alatryste F R 2010 *Chem. Phys.* **375** 464
- [45] Gao T F, Zheng Z G and Chen J C 2016 *J. Phys. A* submitted